

A Functioning Macroscopic “Rubik’s Cube” Assembled via Controllable Dynamic Covalent Interactions

Xiaofan Ji, Zhao Li, Xiaolin Liu, Hui-Qing Peng, Fengyan Song, Ji Qi, Jacky W. Y. Lam, Lingliang Long, Jonathan L. Sessler,* and Ben Zhong Tang*

The dynamic behavior of a macroscopic adhered hydrogel stabilized through controllable dynamic covalent interactions is reported. These interactions involving the cross-linked formation of a hydrogel through reaction of a diacylhydrazine precursor with a tetraformyl partner, increase as a function of time. By using a contact time of 24 h and different compounds with recognized aggregation-induced emission features (AIEgens), it proves possible to create six laminated acylhydrazone hydrogels displaying different fluorescent colors. Blocks of these hydrogels are then adhered into a structure resembling a Rubik’s Cube, a trademark of Rubik’s Brand Limited, (RC) and allowed to anneal for 1 h. This produces a 3·3·3 block (RC) wherein the individual fluorescent gel blocks are loosely adhered to one another. As a consequence, the 13·3 layers making up the RC can be rotated either horizontally or vertically to produce new patterns. Ex situ modification of the RC or application of a chemical stimulus can be used to produce new color arrangements. The present RC structure highlights how the temporal features, strong versus weak adhesion, may be exploited to create smart macroscopic structures.

Patterns have been widely used in many fields due to their ability to capture unique information or encode for specific functions. For example, olfactory patterns can be classified in terms of discrete neuronal network states,^[1] changes in atmospheric circulation patterns can contribute to extreme temperature trends,^[2] analysis of the spatial patterns of residual forest fires can provide information relevant to global deforestation,^[3] and mesoscopic spatiotemporal phase patterns have been correlated with the so-called beta amplitude variations in neuronal local field potentials.^[4] Color-based patterns are of particular interest. They play a key role in selective colorimetric sensor arrays, including ones that have been used to detect various volatile organic chemicals or gases.^[5] Website information can be stored in the form of colored patterns.^[6] Moreover, pattern-based colored materials have found applications in other areas,

Dr. X. Ji, Dr. Z. Li, X. Liu, Dr. H.-Q. Peng, Dr. F. Song, Dr. J. Qi, Prof. J. W. Y. Lam, Prof. B. Z. Tang
Department of Chemistry
Hong Kong Branch of Chinese National Engineering Research Center for Tissue Restoration and Reconstruction and Institute for Advanced Study
The Hong Kong University of Science and Technology (HKUST)
Clear Water Bay, Kowloon, Hong Kong, China
E-mail: tangbenz@ust.hk

Dr. X. Ji, Dr. Z. Li, X. Liu, Dr. H.-Q. Peng, Dr. F. Song, Dr. J. Qi, Prof. J. W. Y. Lam, Prof. B. Z. Tang
HKUST Shenzhen Research Institute
No. 9 Yuexing 1st RD, South Area, Hi-tech Park Nanshan
Shenzhen 518055, China

Prof. L. Long, Prof. J. L. Sessler
Department of Chemistry
The University of Texas at Austin
Austin, TX 78712-1224, USA
E-mail: sessler@cm.utexas.edu

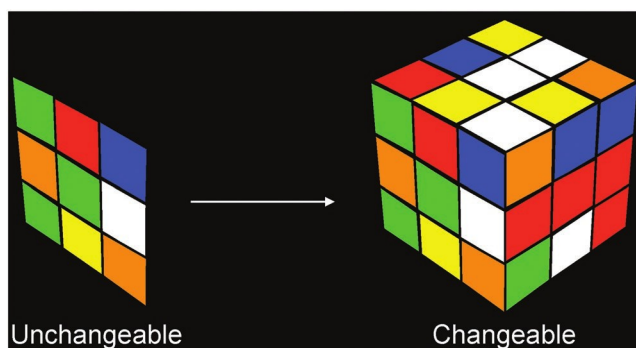
Prof. B. Z. Tang
Center for Aggregation-Induced Emission
SCUT-HKUST Joint Research Institutes
State Key Laboratory of Luminescent Materials and Devices
South China University of Technology
Guangzhou 510640, China

 The ORCID identification number(s) for the author(s) of this article can be found under <https://doi.org/10.1002/adma.201902365>.

DOI: 10.1002/adma.201902365

including structure-based color printing,^[7] oligonucleotide arrays,^[8] electroluminescent devices,^[9] color vision mapping in the human retina,^[10] computational modeling,^[11] memory networks,^[12] and biological mimicry.^[13] In many of these applications, new colored patterns had to be generated so as to realize new/different applications/functions. This is a challenge from a materials perspective since most systems produce patterns that are not interchangeable. A functional, materials-based array system whose pattern can be changed through simple physical manipulation may allow for new advances in pattern-related research and applications. Here we describe such a system modeled after the Rubik’s Cube, a trademark of Rubik’s Brand Limited.

The Rubik’s Cube (RC)^[14] is a plastic toy that is usually made up of 27 small cubes arranged into a larger cube through mechanical locks, three cubes to an edge. Each of the six square faces of the larger cube is colored in one of six eye-catching colors—typically blue, green, yellow, orange, red, and white. Thus, the six color square faces of RC can act as different pattern candidates. Each layer of an RC can be rotated in different directions, resulting in a rearrangement of the pattern on each face. Inspired by this unique aspect of the RC, we sought a chemical means for making an RC-like material wherein the patterns could be changed through simple physical manipulation (**Scheme 1**). To mimic such a structure without relying

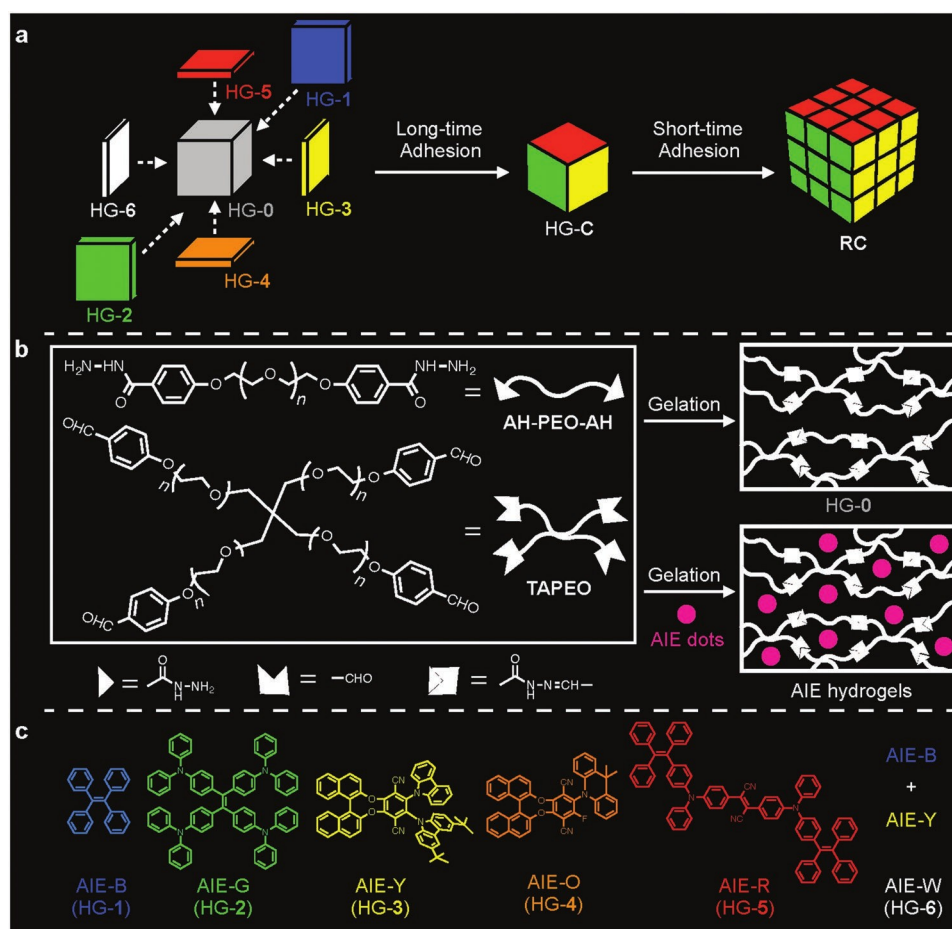


Scheme 1. A Rubik's Cube-like structure allows for the simple creation of a wide range of patterns. The name and representations of the Rubik's Cube are used by permission of Rubik's Brand Ltd.

on mechanical links, we sought to exploit robust yet reversible dynamic interactions^[16–29] between individual colored blocks so as to create an overall hydrogel-based RC-like structure (RC) (**Scheme 2**) that benefits from the special features of the constituent dynamic hydrogel material.^[30] In preparing such a structure, the design of the dynamic covalent interaction

is very important. Overly strong dynamic covalent interactions between hydrogel building blocks will not enable the layers of the RC to be rotated relative to one another. Conversely, dynamic covalent interactions that are too weak will not allow for the formation of a structurally stable RC or its constituent building blocks. In principle, the judicious use of transient differences in hydrogel binding strength may permit both the relatively weak adhesion effects needed to endow an RC with flexibility while providing interactions that are strong enough to enforce its integrity. As detailed below, this design expectation has been realized. In particular, we show that a robust, yet dynamic multicolored, pattern-producing system may be prepared from six hydrogel films containing different aggregation-induced emission (AIE)^[31–34] dots and one hydrogel cube lacking an AIE moiety through macroscopic adhesion. The as-prepared hydrogel RC could then be further modified through both physical and chemical means.

As noted above and shown in Scheme 2, the hydrogel RC was formed using six AIE hydrogels (HG-1 to HG-6) and one hydrogel HG-0 without AIE dots (Scheme 2a). Hydrogel HG-0 is a cube structure while the other AIE hydrogels (HG-1 to HG-6) are thin cuboids with different fluorescent colors. These



Scheme 2. a) Cartoon showing the preparation of a chemical Rubik's Cube (RC) through the macroscopic adhesion of hydrogel HG-0 and AIE hydrogels (from HG-1 to HG-6: blue, green, yellow, orange, red, and white hydrogel, respectively). b) Chemical structures and cartoon representations of the hydrogels used in this study. c) Chemical structures of the AIEgens used in this study. The name and representations of the Rubik's Cube are used by permission of Rubik's Brand Ltd.

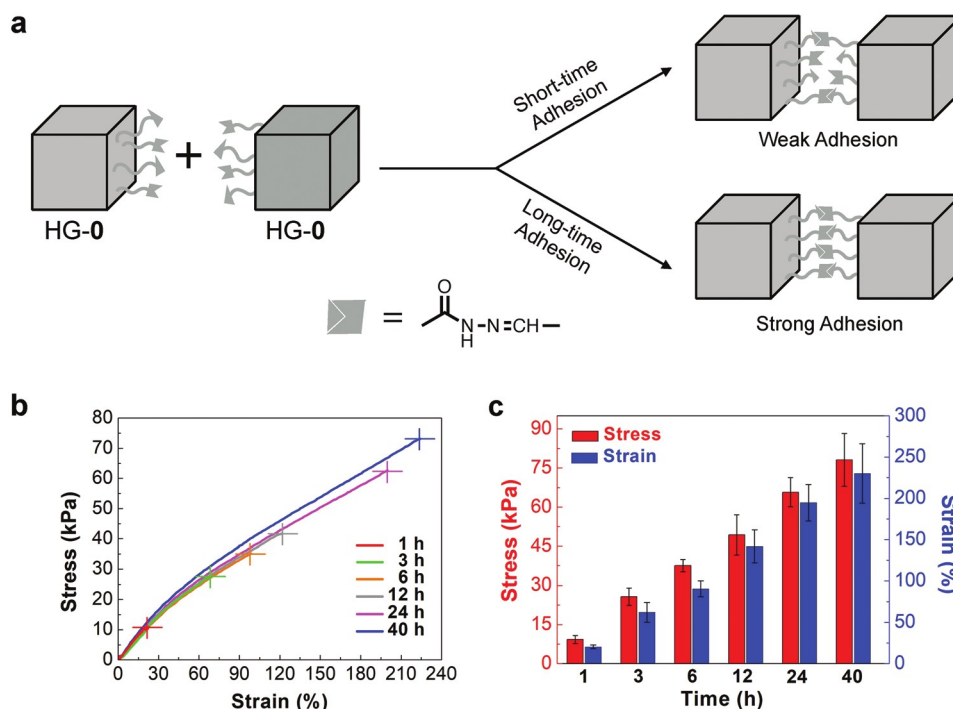


Figure 1. a) Cartoon representation of the time-dependent macroscopic adhesion of two hydrogels HG-0. b) Tensile behavior of the resulting two-block model (dumbbell shaped) macroscopic adhesion as a function of differing adhesion times ranging from 1 to 40 h, with corresponding nominal stress plotted against strain. c) Adhesion time dependence of the associated fracture stress and fracture strain.

seven hydrogels were first macroscopically adhered into an integral cube hydrogel HG-C by exploiting interfacial dynamic covalent interactions. The resulting cubes were allowed to set for 24 h (i.e., long-time adhesion), to enforce strong interfacial adhesion. Next, individual blocks of hydrogel HG-C itself were macroscopically adhered to produce the target RC, which was only allowed to set for roughly 1 h. This provides for only weak interfacial adhesion (cf. **Figure 1**).

Hydrogels HG-0 – HG-6 were produced from two polymers: acylhydrazine-terminated PEO (AH-PEO-AH) and tetraaldehyde-terminated PEO (TAPEO) (Scheme 2b). The synthesis and characterization of these two polymers, which have precedents in the literature,^[30,35–37] and the requisite AIEgens, also previously described,^[38–40] are detailed in Figures S1–S18 (Supporting Information). Their combination in the present context is, however, new. Thus, hydrogel HG-0 was formed by mixing these two polymers in aqueous solution, while AIE hydrogels (HG-1 to HG-6) were produced by mixing the two polymers in aqueous suspensions of AIE dots (Scheme 2b). Due to the presence of the AIEgens,^[43–47] the six AIE hydrogels (HG-1 to HG-6) produced different fluorescent colors upon UV illumination (cf. **Figure 2**).

When these hydrogels are placed in contact, the acylhydrazone bonds of one hydrogel interact with those of another hydrogel.^[30,48,49] Over short times (e.g., 1 h) only a small percentage of the acylhydrazone bonds undergo exchange leading to a low level of stickiness. With increasing time, stronger and more interfacial interactions are expected. Support for this postulate came from studies^[37] wherein two HG-0 hydrogels of same weight were assembled and tested in a time-dependent manner between the surfaces, two gels, G-9 and G-10, were subjected to an additional adhesion test (Scheme S1, Supporting

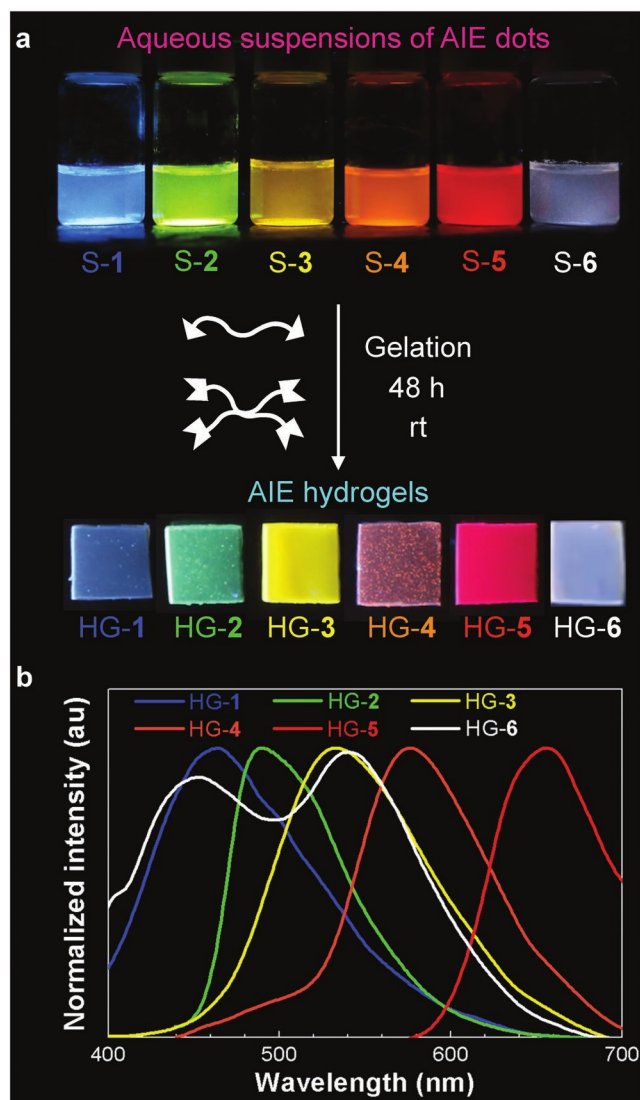


Figure 2. a) Photographs of aqueous suspensions of AIE dots (from S-1 to S-6: blue, green, yellow, orange, red, and white suspensions, respectively) and the corresponding AIE hydrogels (HG-1 to HG-6). b) Fluorescent spectra of the latter hydrogels.

Information). The AIE-YG-containing gel G-9 gives rise to a bright fluorescence due to the AIE effect of the constituent tetraphenylethene (TPE)^[33,34]. In contrast, G-10 lacks an AIEgen and displays little appreciable fluorescence. When these two gels were adhered together the groups of G-9 at the surface, exchange into gel G-10 due to the dynamic nature of the acylhydrazone bonds present at the interfaces. This exchange converts the initially nonfluorescent gel G-10 into a fluorescent material (Scheme S1, Supporting Information). As the adhesion time increases, a greater number of acylhydrazone bonds exchange. The fluorescent emission intensity of gel G-10 thus likewise increases with time (Figures S29 and S30, Supporting Information). A series of gels with different AIE-YG concentrations was also prepared. These systems were used to confirm the expected relationship between gel fluorescent intensity and AIE-YG concentration

(Figures S31 and S32, Supporting Information). This was taken as additional evidence that acylhydrazone bonds exchange at the interface and do so in a time-dependent manner (Figure S33, Supporting Information).

The above temporal features led us to consider that it might be possible to produce a functioning Rubik's Cube (RC)-like structure (i.e., RC; Scheme 2).

To create an RC mimic using soft materials, we first prepared a small cube, HG-C with six separate AIEgen colored faces (cf. **Figure 3a** and Movie S2 of the Supporting Information). Hydrogel HG-C was allowed to set for 24 h. This allowed for robust adhesion between the core hydrogel and the colored faces. With HG-C in hand, 27 HG-C blocks were adhered in a $3 \times 3 \times 3$ arrangement. After a relatively short adhesion time, 1 h, RC was formed in stable fashion (Figure 3b and Movie S3 of the Supporting Information). No disassembly or dispersion of the component hydrogels or AIEs was observed when RC was subject to gentle shaking or when repeatedly lifted up, thrown down, or turned over (cf. Figure 3c and Movie S4 of the Supporting Information).

Individual $1 \times 3 \times 3$ layers within an RC may be rotated to change the pattern on each face and hence the cube as a whole. It was thus of interest to explore whether the presumed dynamic features of RC would permit such rotations (cf. **Figure 4**; cartoon representations on the left and photographs on the right). As shown in Figure 4a and Movie S5 of the Supporting Information, when the top $1 \times 3 \times 3$ layer of RC is rotated horizontally 90° in a counterclockwise direction, the front face pattern P1 is transformed into pattern P2. The top two layers of RC were then rotated horizontally 180° clockwise direction; this changed the front face from pattern P2 to P3. A subsequent horizontal 90° rotation in a counterclockwise direction produced pattern P0 on the front face. The horizontal rotation-induced pattern transformation reflects the difference of adhesion strength between hydrogels: The relatively weak adhesion enables the RC to be rotated horizontally, while the strong interactions allow HG-C to be used as a stable (i.e., nondynamic) building block. Pattern transformations by vertical rotation were also investigated (Figure 4b; Movie S6, Supporting Information). For instance, rotating the middle and right two layers of RC vertically 90° in a counterclockwise direction served to change the front face pattern from P4 to P5. A subsequent vertical 90° rotation in a counterclockwise direction involving only the rightmost $1 \times 3 \times 3$ layer served to convert pattern P5 to P0'. The vertical rotation-induced pattern transformation thus likewise reflects the binding difference between hydrogels; again, the relatively weak adhesion enables the RC to be rotated vertically, while the strong interactions allow HG-C to be used as a stable building block.

The layers making up RC could also be rotated both horizontally and vertically in a concerted fashion (Figure 4c and Movie S7 of the Supporting Information). For instance, the right layer of RC could be rotated vertically 90° in a counterclockwise direction (causing the front face from pattern P6 to pattern P7). Then, the top layer of RC could be rotated horizontally 90° in a counterclockwise direction to convert the front face from pattern P7 to pattern P0'. On the basis of this observation, we conclude that the relatively weak adhesion between (as opposed to within) individual building blocks could be exploited to produce an all-

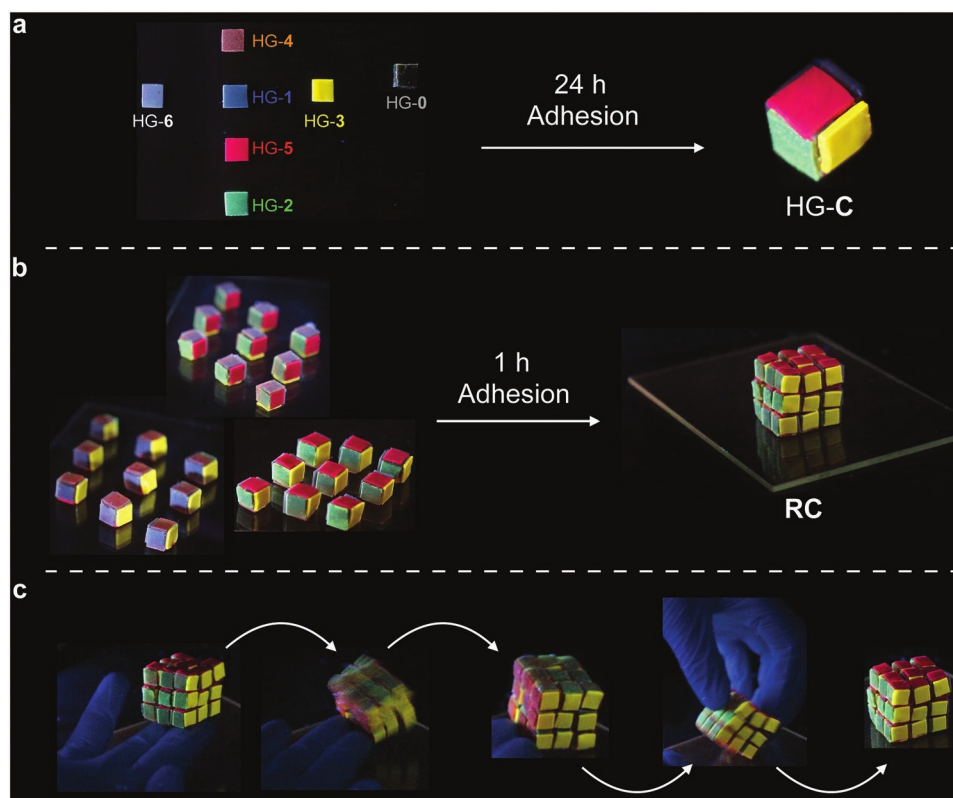


Figure 3. Photographs showing a) the formation of hydrogel HG-C via the macroscopic adhesion of hydrogel HG-0 and AIE hydrogels HG-1 – HG-6 with annealing for 24 h, b) the formation of a Rubik's Cube-like hydrogel RC through the macroscopic adhesion of individual hydrogel HG-C blocks ($3 \cdot 3 \cdot 3$) and allowing to set for 1 h, and c) hydrogel RC being rolled by hand. The size of hydrogel HG-0 is 88 mm^3 . The AIE hydrogel layers (i.e., HG-1 – HG-6) are all $8 \cdot 8 \cdot 1 \text{ mm}^3$. The name and representations of the Rubik's Cube are used by permission of Rubik's Brand Ltd.

hydrogel-based RC system whose layers may be rotated freely in both the horizontal and vertical direction.

The pattern transformations engendered within RC by mechanical means are made possible by the time-dependent control over the dynamic covalent interactions at the hydrogel interfaces, which in turn reflects the time-dependent adhesion features of the underlying hydrogels. Specifically, the relatively weak adhesion that characterizes the intracube interactions within the RC stand in contrast to the strong interactions that allow HG-C to be used as a robust block to prepare the $3 \cdot 3$ RC structure.

In contrast to what is true for traditional hard plastic Rubik's Cube, RC is comprised of a soft material. Therefore, besides rotation, its patterns may be changed by other means. In fact, it proved possible to remove one cube HG-C from RC. The free HG-C cube can be rotated freely and then inserted back into the resulting gap to produce an intact RC but with a pattern that differs at three faces (Figure 5a; Movie S8, Supporting Information). Such an ex situ pattern transformation is not easily achieved with a traditional Rubik's Cube without risk of breakage. Furthermore, and again in contrast to what is true for a traditional Rubik's Cube, the fluorescent AIEgen color may be changed by treatment with an appropriate chemical stimulus. For example, AIE-RB is a blue fluorophore; however, the color of its fluorescent emission changes to orange after treatment with acid (Figure S34, Supporting Information).

Another hydrogel, HG-7, containing AIE-RB was thus prepared; as expected, it was found to change from blue to orange over the course of 8 min upon exposure to acetic acid (Movie S9 and Figure S34, Supporting Information). This chemical stimulus-based color change was recapitulated in an RC structure containing one HG-7 bearing HG-C block (Figure 5b; Movie S10, Supporting Information). This indicates the environment-induced change of the RC face pattern. Finally, we found that the $3 \cdot 3 \cdot 3$ RC structure can be divided physically to produce daughter products (including a $2 \cdot 2 \cdot 2$ RC structure) that can be re-fused to create the original RC pattern or a different one (Figure 5c; Movie S11, Supporting Information). This transformation between the starting $3 \cdot 3 \cdot 3$ RC and the daughter $2 \cdot 2 \cdot 2$ RC structure means that the size of the patterns changes. This provides a further complement to pattern production involving layer rotation, individual cube manipulation, and chemical treatment. This diversity is to our knowledge unique in the context of a materials-based colored array system. In addition, according to previous studies, hydrogel materials can also be adhered to other normalized interactive surface areas.^[51–53] A number of parameters, including surface roughness, wettability, and surface group density, are known to influence the macroscopic assembly and interaction results.^[41,56] We also note that the transient differences in the binding strength between the individual hydrogel building blocks and within the assembled RC are of interest in the context of soft materials. In

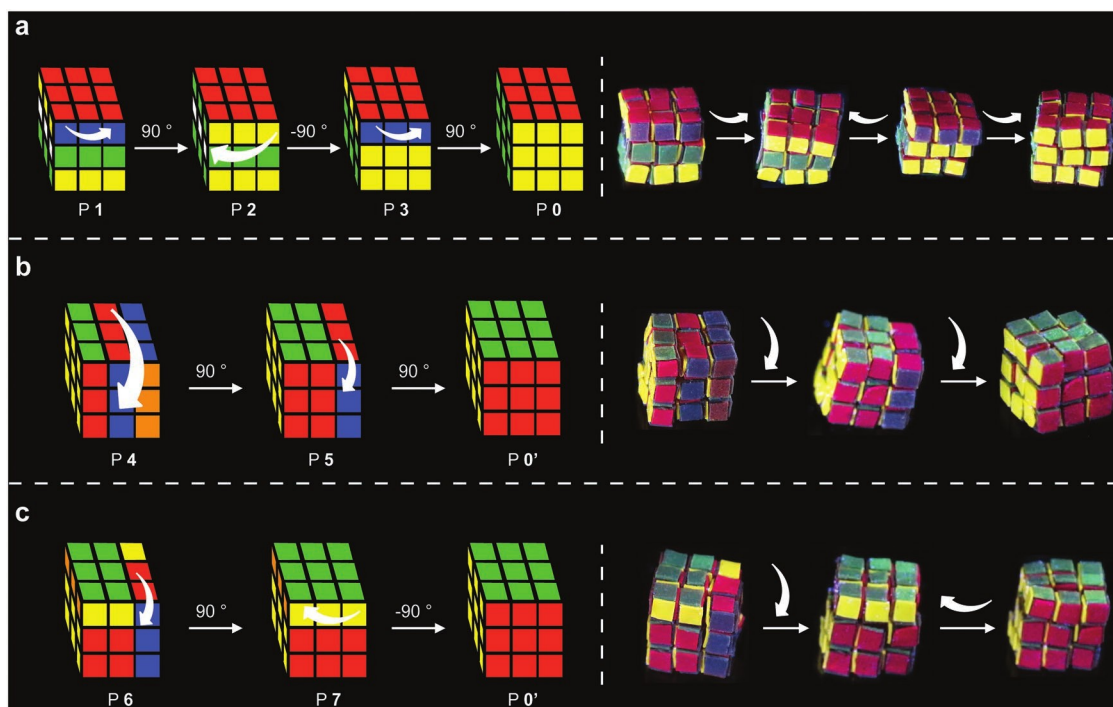


Figure 4. Pattern transformation by a) horizontally rotating layers within hydrogel RC, b) vertically rotating layers within hydrogel RC, and c) rotating layers within hydrogel RC both horizontally and vertically. Cartoon representations on the left and photographs on the right. The name and representations of the Rubik's Cube are used by permission of Rubik's Brand Ltd.

line with a recent suggestion from Whitesides, we specifically propose that systems such as described here may have a role play in the preparation of soft robotics.^[57]

In conclusion, we prepared six AIE hydrogels showing different fluorescent colors and one hydrogel without an AIE dot. These seven hydrogels were used to create a cube structure,

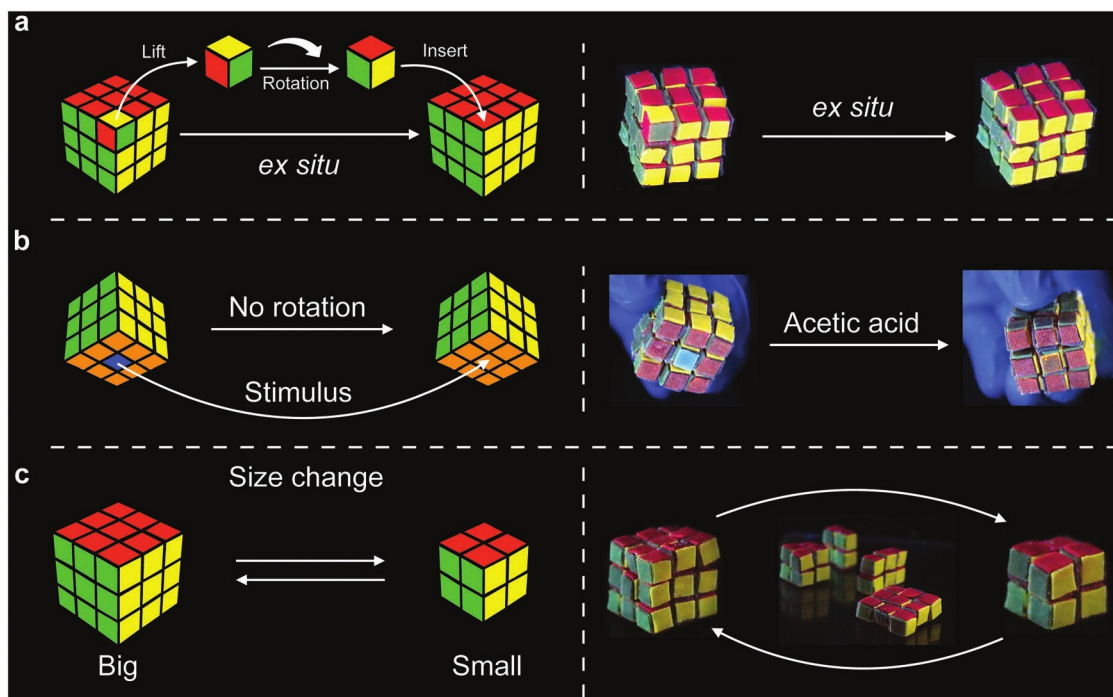


Figure 5. Change in the RC face pattern a) produced via *ex situ* modification, b) induced by a chemical stimulus, and c) through changes in the size of the RC. The name and representations of the Rubik's Cube are used by permission of Rubik's Brand Ltd.

hydrogel HG-C, bearing different AIE-based colored faces. Macroscopic adhesion of 27 of these HG-C building blocks with a short adhesion time (≈ 1 h) then allowed preparation of a Rubik's Cube-like structure RC. Due to the dynamic nature of the contacts between the HG-C blocks within RC, physically driven changes to the structure and patterns of RC proved possible. In addition, ex situ or chemical stimulus approaches could be exploited to alter the RC color patterns. An attractive feature of the present RC structure is that it allows for the facile creation of multiple patterns. As such, it could see potential application in areas where pattern-dependent behavior could prove beneficial. On a more fundamental level, this study highlights how the temporal features, strong versus weak adhesion, of dynamic covalent hydrogels may be exploited to create easy-to-manipulate macroscopic structures.

Supporting Information

Supporting Information is available from the Wiley Online Library or from the author.

Acknowledgements

X.J. and Z.L. contributed equally to this work. The authors thank Prof. Zi Liang Wu (Department of Polymer Science and Engineering, Zhejiang University) for his kind help with the revisions to this manuscript. B.Z.T. acknowledges the financial support from the National Science Foundation of China (21788102, 21490570, and 21490574), the Research Grant Council of Hong Kong (16308116 and C6009-17G), the Science and Technology Plan of Shenzhen (JCYJ20160229205601482, JCYJ20170307173739739 and JCYJ20170818113602462) and the Innovation and Technology Commission (ITC-CNERC149C01). J.L.S. acknowledges financial support from the National Science Foundation (CHE CHE-1807152) and the Robert A. Welch Foundation (F-0018). The name and representations of the Rubik's Cube are used by permission of Rubik's Brand Ltd.

Conflict of Interest

The authors declare no conflict of interest.

Keywords

aggregation-induced emission, dynamic covalent interactions, fluorescence, hydrogel, pattern

Received: April 12, 2019
Revised: June 25, 2019
Published online: August 7, 2019

- [1] J. Niessing, R. W. Friedrich, *Nature* **2010**, 465, 47.
- [2] D. E. Horton, N. C. Johnson, D. Singh, D. L. Swain, B. Rajaratnam, N. S. Dissenbaugh, *Nature* **2015**, 522, 465.
- [3] F. Taubert, R. Fischer, J. Groeneveld, S. Lehmann, M. S. Müller, E. Rodig, T. Wiegand, A. Huth, *Nature* **2018**, 554, 519.
- [4] M. Denker, L. Zehl, B. E. Kilavik, M. Diesmann, T. Brochier, A. Riehle, S. Grun, *Sci. Rep.* **2018**, 8, 5200.
- [5] J. H. Lee, B. Fan, T. D. Samdin, D. A. Monteiro, M. S. Desai, O. Scheideler, H. E. Jin, S. Kim, S. W. Lee, *ACS Nano* **2017**, 11, 3632.
- [6] D. H. Park, C. J. Han, Y. G. Shul, J. H. Choy, *Sci. Rep.* **2015**, 4, 4879.
- [7] H. Kim, J. P. Ge, J. Kim, S. Choi, H. Lee, H. Lee, W. Park, Y. Yin, S. Kwon, *Nat. Photonics* **2009**, 3, 534.
- [8] R. Kumar, S. Weigel, R. Meyer, C. M. Niemeyer, H. Fuchs, M. Hirtz, *Chem. Commun.* **2016**, 52, 12310.
- [9] S. Song, H. Shim, S. K. Lim, S. M. Jeong, *Sci. Rep.* **2018**, 8, 3331.
- [10] R. Sabesan, B. P. Schmidt, W. S. Tuten, A. Roorda, *Sci. Adv.* **2016**, 2, e1600797.
- [11] Y. Fang, V. V. Yashin, S. P. Levitan, A. C. Balazs, *Sci. Adv.* **2016**, 2, e1601114.
- [12] P. M. Sheridan, F. X. Cai, C. Du, W. Ma, Z. Y. Zhang, W. D. Lu, *Nat. Nanotechnol.* **2017**, 12, 784.
- [13] M. Yang, C. Fehl, K. V. Lees, E. K. Lim, W. A. Offen, G. J. Davies, D. J. Bowles, M. G. Davidson, S. J. Roberts, B. G. Davis, *Nat. Chem. Biol.* **2018**, 14, 1109.
- [14] I. Kriz, P. Siegel, *Sci. Am.* **2008**, 299, 84.
- [15] V. Rich, *Nature* **1982**, 295, 361.
- [16] N. Bowden, A. Terfort, J. Carbeck, G. M. Whitesides, *Science* **1997**, 276, 233.
- [17] A. Harada, R. Kobayashi, Y. Takashima, A. Hashidzume, H. Yamaguchi, *Nat. Chem.* **2011**, 3, 34.
- [18] C. Ma, T. Li, Q. Zhao, X. Yang, J. Wu, Y. Luo, T. Xie, *Adv. Mater.* **2014**, 26, 5665.
- [19] X. Z. Yan, D. H. Xu, X. D. Chi, J. Z. Chen, S. Y. Dong, X. Ding, Y. H. Yu, F. H. Huang, *Adv. Mater.* **2012**, 24, 362.
- [20] M. Cheng, F. Shi, J. Li, Z. Lin, C. Jiang, M. Xiao, L. Zhang, W. Yang, T. Nishi, *Adv. Mater.* **2014**, 26, 3009.
- [21] X. Ji, R. T. Wu, L. Long, X. S. Ke, C. Guo, Y. J. Ghang, V. M. Lynch, F. Huang, J. L. Sessler, *Adv. Mater.* **2018**, 30, 1705480.
- [22] G. Ju, F. Guo, Q. Zhang, A. J. Kuehne, S. Cui, M. Cheng, F. Shi, *Adv. Mater.* **2017**, 29, 1702444.
- [23] Q. Li, Y. W. Zhang, C. F. Wang, D. A. Weitz, S. Chen, *Adv. Mater.* **2018**, 30, 1803475.
- [24] Q. Wu, P. M. Rauscher, X. L. Lang, R. J. Wojtecki, J. J. de Pablo, M. J. A. Hore, S. J. Rowan, *Science* **2017**, 358, 1434.
- [25] H. Wang, X. F. Ji, Z. T. Li, F. H. Huang, *Adv. Mater.* **2017**, 29, 1606117.
- [26] J. Li, Z. Xu, Y. Xiao, G. Gao, J. Chen, J. Yin, J. Fu, *J. Mater. Chem. B* **2018**, 6, 257.
- [27] L. J. Chen, H. B. Yang, *Acc. Chem. Res.* **2018**, 51, 2699.
- [28] G. Ju, M. Cheng, F. Guo, Q. Zhang, F. Shi, *Angew. Chem., Int. Ed.* **2018**, 57, 8963.
- [29] W. Zheng, W. Wang, S. T. Jiang, G. Yang, Z. Li, X. Q. Wang, G. Q. Yin, Y. Zhang, H. W. Tan, X. P. Li, H. M. Ding, G. S. Chen, H. B. Yang, *J. Am. Chem. Soc.* **2019**, 141, 583.
- [30] G. H. Deng, C. M. Tang, F. Y. Li, H. F. Jiang, Y. M. Chen, *Macromolecules* **2010**, 43, 1191.
- [31] J. D. Luo, Z. L. Xie, J. W. Y. Lam, L. Cheng, H. Y. Chen, C. F. Qiu, H. S. Kwok, X. W. Zhan, Y. Q. Liu, D. B. Zhu, B. Z. Tang, *Chem. Commun.* **2001**, 1740.
- [32] J. Mei, Y. N. Hong, J. W. Y. Lam, A. J. Qin, Y. H. Tang, B. Z. Tang, *Adv. Mater.* **2014**, 26, 5429.
- [33] J. Mei, N. L. C. Leung, R. T. K. Kwok, J. W. Y. Lam, B. Z. Tang, *Chem. Rev.* **2015**, 115, 11718.
- [34] H. T. Feng, Y. X. Yuan, J. B. Xiong, Y. S. Zheng, B. Z. Tang, *Chem. Soc. Rev.* **2018**, 47, 7452.
- [35] G. H. Deng, F. Y. Li, H. X. Yu, F. Y. Liu, C. Y. Liu, W. X. Sun, H. F. Jiang, Y. M. Chen, *ACS Macro Lett.* **2012**, 1, 275.
- [36] Z. Li, Z. Zheng, S. Su, L. Yu, X. Wang, *Macromolecules* **2016**, 49, 373.
- [37] F. Liu, F. Li, G. Deng, Y. Chen, B. Zhang, J. Zhang, C.-Y. Liu, *Macromolecules* **2012**, 45, 1636.
- [38] K. Li, W. Qin, D. Ding, N. Tomczak, J. L. Geng, R. R. Liu, J. Z. Liu, X. H. Zhang, H. W. Liu, B. Liu, B. Z. Tang, *Sci. Rep.* **2013**, 3, 1150.

- [39] F. Y. Song, Z. Xu, Q. S. Zhang, Z. Zhao, H. K. Zhang, W. J. Zhao, [47] J. S. Ni, P. F. Zhang, T. Jiang, Y. C. Chen, H. F. Su, D. Wang, Z. J. Qiu, C. X. Qi, H. Zhang, H. H. Y. Sung, I. D. Williams, Z. Q. Yu, R. T. K. Kwok, Z. J. Zhao, J. W. Y. Lam, B. Z. Tang, J. W. Y. Lam, Z. J. Zhao, A. J. Qin, D. G. Ma, B. Z. Tang, *Adv. Mater.* **2018**, *30*, 1805220.
- [40] L. F. Zhao, Y. L. Lin, T. Liu, H. X. Li, Y. Xiong, W. Z. Yuan, [48] R. J. Wojtecki, M. A. Meador, S. J. Rowan, *Nat. Mater.* **2011**, *10*, 14.
- [41] Y. N. Lin, C. Y. Li, G. S. Song, C. C. He, Y. Q. Dong, H. L. Wang, [49] M. Burnworth, L. M. Tang, J. R. Kumpfer, A. J. Duncan, F. L. Beyer, G. L. Fiore, S. J. Rowan, C. Weder, *Nature* **2011**, *472*, 334.
- [42] H. Y. Zheng, C. Y. Li, C. C. He, Y. Q. Dong, Q. S. Liu, P. F. Qin, [50] M. Wang, Y. R. Zheng, K. Ghosh, P. J. Stang, *J. Am. Chem. Soc.* **2019**, *132*, 6282.
- [43] Y. S. Li, A. D. Shao, Y. Wang, J. Mei, D. C. Niu, J. L. Gu, [51] Y. Takashima, T. Sahara, T. Sekine, T. Kakuta, M. Nakahata, M. Takahata, T. Nonoyama, T. Nakajima, J. P. Gong, *Adv. Mater.* **2015**, *27*, 7344.
- [44] Y. H. Cheng, J. G. Wang, Z. J. Qiu, X. Y. Zheng, N. L. C. Leung, [52] S. K. Roy, H. L. Guo, T. L. Sun, A. B. Ihsan, T. Kurokawa, M. Takahata, T. Nonoyama, T. Nakajima, J. P. Gong, *Adv. Mater.* **2015**, *27*, 7344.
- [45] J. L. Han, J. You, X. G. Li, P. F. Duan, M. H. Liu, *Adv. Mater.* **2017**, *29*, 1606503.
- [46] Z. H. Sheng, B. Guo, D. H. Hu, S. D. Xu, W. B. Wu, W. H. Li, [53] J. Liu, O. A. Scherman, *Adv. Funct. Mater.* **2018**, *28*, 1800848.
- [47] J. S. Ni, P. F. Zhang, T. Jiang, Y. C. Chen, H. F. Su, D. Wang, [54] M.-J. Cheng, Q. Zhang, F. Shi, *Chin. J. Polym. Sci.* **2018**, *36*, 306.
- [48] R. J. Wojtecki, M. A. Meador, S. J. Rowan, *Nat. Mater.* **2011**, *10*, 14.
- [49] M. Burnworth, L. M. Tang, J. R. Kumpfer, A. J. Duncan, F. L. Beyer, [55] G. Ju, M. Cheng, Q. Zhang, F. Guo, P. Xie, F. Shi, *ACS Appl. Nano Mater.* **2018**, *1*, 5662.
- [50] M. Wang, Y. R. Zheng, K. Ghosh, P. J. Stang, *J. Am. Chem. Soc.* **2019**, *132*, 6282.
- [51] Y. Takashima, T. Sahara, T. Sekine, T. Kakuta, M. Nakahata, [56] R. Akram, M. Cheng, F. Guo, S. Iqbal, F. Shi, *Langmuir* **2016**, *32*, 3617.
- [52] S. K. Roy, H. L. Guo, T. L. Sun, A. B. Ihsan, T. Kurokawa, [57] G. M. Whitesides, *Angew. Chem., Int. Ed.* **2018**, *57*, 4258.